Usage-based Lifing of Lithium-Ion Battery with Hybrid Physics-Informed Neural Networks

Renato G. Nascimento*, Felipe A. C. Viana†
University of Central Florida, Orlando, FL, 32816, USA

Matteo Corbetta‡ Chetan S. Kulkarni§
KBR LLC, NASA Ames Research Center, Moffett Field 94035 CA, USA

Lithium-ion batteries are commonly used to power unmanned aircraft vehicles (UAVs). The ability to model and forecast the remaining useful life of these batteries enables UAV reliability assurance. Building accurate models for battery state of charge and state of health based on first principles is challenging due to the complex electrochemistry that governs battery operations and computational complexity required to solve them. Therefore, reduced order models are often used due to their ability to capture the overall battery discharge. Unfortunately, these simplifications lead to residual discrepancy between model predictions and observed data. In this paper, we present a hybrid modeling approach merging reduced-order models and neural networks. In this approach, while most of the input-output relationship is captured by Nernst and Butler-Volmer equations, data-driven kernels reduce the gap between predictions and observations. We validate our approach using data publicly available through the NASA Prognostics Center of Excellence repository. Results showed that our hybrid battery prognosis model can be successfully calibrated, even with a limited number of observations.

I. Nomenclature

Λ	=	Loss function
MLP	=	Multi-layer perceptron
RNN	=	Recurrent neural network
D	=	Diffusion constant
F	=	Faraday constant
J_i	=	Current density
$J_{i,0}$	=	Exchange current density
R	=	Universal gas constant
R_0	=	Lumped internal resistance
T	=	Electrode temperature
U	=	Potential
V	=	Voltage
$\boldsymbol{b}$	=	Neural network model bias vector
c	=	Li-ion concentration
i	=	Current
m	=	Number of Electrons transferred during reaction
n	=	Sub-script of negative electrode
p	=	Sub-script of positive electrode
q	=	Charge, available Li-ions
$\mathbf{u}$	=	Battery input vector
x	=	Mole fraction
$\mathbf{y}$	=	Battery observable state vector

*Graduate Research Assistant, Department of Mechanical and Aerospace Engineering, renato.gn@knights.ucf.edu, AIAA Student Member.
†Assistant Professor, Department of Mechanical and Aerospace Engineering, viana@ucf.edu, Sr. AIAA Member.
‡Research Engineer, matteo.corbetta@nasa.gov, AIAA Member.
§Research Engineer, chetan.s.kulkarni@nasa.gov, Sr. AIAA Member.

II. Introduction

Lithium-ion batteries are commonly used to power electric unmanned aircraft vehicles (UAVs) [1--3]. Therefore, the ability to model both the state of charge as well as battery health is very important for reliable and affordable operation of UAV fleets. Even though models based on first principles are accurate and trustworthy, the complex electro-chemistry that governs battery operation makes it hard to build and use such models for in-time monitoring of battery conditions. Moreover, the careful tuning or estimation of high-fidelity model parameters hamper the straightforward deployment in the field. Reduced order models and machine learning models present computationally tractable alternatives to high-fidelity physics-based simulations, they can be run on-board relatively small vehicles at the cost of lower precision.

Reduced-order physics-based models are built by carefully simplifying the physics such that computational cost is dramatically reduced while maintaining the ability to describe the system main dynamic behavior. This approach can lead to a number of parameters to be estimated based on data as well as residual model-form uncertainty; a property shared with machine learning models. The latter are solely built on the basis of data, and can capture unexpected nonlinearities. The drawback is that traditional machine learning tends to require large number of data points hard to retrieve in many scientific and engineering fields like, for example, the field of battery discharge and degradation prediction.

In this paper, we use a hybrid modeling approach for battery usage-based lifing that directly implements physics kernels within deep neural networks. We leverage a reduced-order physics-based model for battery state of charge developed in [4, 5]. Then, we pair this model with data-driven kernels in order to reduce the gap between predictions and observations as well as to perform uncertainty quantification. The numerical integration of the resulting time-dependent state space model is performed with a recurrent neural network [6--9].

The developed approach is validated using data publicly available through the NASA Prognostics Center of Excellence repository [10, 11]. This data set contains a collection of reference discharge (constant loading) cycles as well as random discharge cycles for a set of eight Li-ion batteries. Results showed that our hybrid battery usage-based lifing model can be successfully calibrated with data from this small population of batteries. Moreover, the model can help optimizing battery operation by offering long-term forecast of battery capacity.

The remaining of the paper is organized as follows. Section III gives an overview on the reduced-order battery discharge model and presents our proposed physics-informed neural network model. Section IV describes in detail our main results including model fitting and validation as well as random-loading discharge predictions. Finally, section V concludes the paper by summarizing significant remarks, and providing insight on potential future studies.

III. Hybrid Physics-Informed Neural Networks for Lithium-Ion Battery Lifing

A. Reduced-order Physics-based Model

We adopted the electro-chemistry surrogate model proposed in [4], which mixes physics-derived and empirical equations, and was originally proposed for real-time applications. It relies on ordinary differential equations rather than partial differential equations, making it computationally efficient. Here, we report only a summary of the model. The interested reader is referred to [4] for more details and a thorough description.

The model uses Nernst's equation for the equilibrium potential:

$$V_{U,i} = U_0 + \frac{R\,T}{m\,F} \ln \frac{1 - x_i}{x_i} + V_{int,i}\,, \tag{1}$$

where: i indicates the subscript of the electrode (negative n or positive p); R is the universal gas constant; T is the electrode temperature; m is the number of electrons transferred in the reaction; F is the Faraday constant; x is the mole fraction for the Lithium-intercalated host material; U_0 is the reference potential; and V_{int} is the internal voltage and activity correction term, null in ideal conditions. Details about V_{int} will be provided later in the section. The mole fraction is computed as the ratio between the amount of Li-ion q in electrode $i = \{n, p\}$, and the amount of available (moving) Li-ions q^{max}:

$$x_i = \frac{q_i}{q^{max}}\,, \qquad \text{and} \qquad q^{max} = q_n + q_p\,. \tag{2}$$

In order to accommodate the concentration gradient at the surface of the electrode, the total volume of the battery is

split into two control volumes, bulk v_b and surface v_s, and the concentrations of Li-ions are calculated accordingly:

$$c_{b,i} = \frac{q_{b,i}}{v_{b,i}}\,, \qquad c_{s,i} = \frac{q_{s,i}}{v_{s,i}}\,. \tag{3}$$

The number of Li-ions in the different volumes must satisfies the following equalities: $q_p = q_{s,p} + q_{b,p}$, $q_n = q_{s,n} + q_{b,n}$, as well as the second equality in Eq. (2). The diffusion rate from the bulk to the surface is:

$$\dot{q}_{b\,s,i} = \frac{1}{D}\left(c_{b,i} - c_{s,i}\right), \tag{4}$$

where D is the diffusion constant. The equations for the rates of change of the charges q are not reported from the sake of brevity and can be retrieved in [4]. The concentration overpotential is calculated using the Nernst's equation for the surface, which is by substituting x_i with $x_{s,i}$:

$$x_{s,i} = \frac{q_{s,i}}{q^{max}_{s,i}}\,, \qquad \text{and} \qquad q^{max}_{s,i} = q^{max}\,\frac{v_{s,i}}{v_i}\,. \tag{5}$$

The solid-phase Ohmic resistance, electrolyte Ohmic resistance, and current collector resistance can be lumped together into R_0 to calculate the voltage drop: $V_0 = i_{app}\,R_0$, where i_{app} is the required current [4].

The surface overpotential is represented by the Butler-Volmer equation [4], which for Li-ion batteries can be expressed in terms of voltage V_η:

$$V_{\eta,i} = \frac{RT}{F\alpha}\,\text{arcsinh}\left(\frac{J_i}{2J_{i0}}\right), \tag{6}$$

where J_i and J_{i0} are the current density and exchange current density, defined in [4]. This way, the battery output voltage is defined by:

$$V = V_{U,p} - V_{U,n} - V_0 - V_{\eta,p} - V_{\eta,n}\,, \tag{7}$$

which will serve as output of the physics-informed model.

As part of the simplifications used to obtain the described reduced-order physics-based model, we selected the internal voltage V_{int}, battery resistance R_0, and amount of available Li-ions q^{max} as trainable elements of the hybrid framework. As already mentioned, the internal voltage is the activity correction term needed to compute V_U.

Focusing on V_{int}, the model in [4, 5] fits the experimental data using the Redlich-Kister expansion:

$$V_{int,i}(x_i;\,\mathbf{A}_i) = \frac{1}{m\,F}\sum_{k=0}^{N_i} A_{k,i}\left((2x_i-1)^{k+1} + -\frac{2x_i k\,(1-x_i)}{(2x_i-1)^{1-k}}\right). \tag{8}$$

The mole fraction x_i is the independent variable, the coefficients $A_{k,i}$ are identified through data-fitting, and the number of elements in the sum N_i is empirically-derived as well. For the batteries tested in this work, the reference papers [4, 5] kept $N_p = 12$ and $N_n = 0$, thus using a constant internal voltage for the negative side of the electrode.

The rationale behind our selection of the trainable elements is the following. The model prediction performance heavily depends on the lumped internal resistance, R_0, and maximum number of available Li-ions, q^{max}. Such influence appears at both the *inter-* and the *intra*-specimen level; those two parameters change as a battery ages. The loss in active material can be represented by a drop in q^{max}, while an increase in R_0 is representative of a constant Ohmic drop, which causes an increase in total resistance independent of the battery charge state [12]. Such effects should be accounted for when training on multiple discharge curves of the same battery type. Moreover, different samples of the same fleet of batteries also have slightly different R_0 and q^{max}, thus varying from one battery to another and contributing to inter-specimen variability. The selection of the internal voltage came naturally as the surrogate model already makes use of a numerical interpolation technique to provide an estimate of V_{int}. The Redlich-Kister expansion is substituted with a machine learning model that is not restricted by the equation form and can provide uncertainty estimates of the model parameters, as described later in the paper.

B. Physics-Informed Neural Network Model

Our proposed approach for modeling the time-dependent battery state of charge is based on recurrent neural networks (RNNs). RNNs [13--15] differ from traditional feed forward networks, as they are designed to handle time-dependent responses. At every time step t, recurrent neural networks apply a transformation to a state $\mathbf{y}$ such that:

$$[\mathbf{y}_t \quad \mathbf{h}_t]^\top = f(\mathbf{u}_t, \mathbf{y}_{t-1}, \mathbf{h}_{t-1})\,, \tag{9}$$

where the subscript t represents the time discretization index, $\mathbf{y} \in \mathbb{R}^{n_y}$ are the observable states, $\mathbf{h} \in \mathbb{R}^{n_h}$ are the internal states, $\mathbf{u} \in \mathbb{R}^{n_u}$ are input variables, and $f(\cdot)$ defines the transition between time steps (function of input variables and previous states).

While typical RNN architectures are trained solely from data, such as the long-short term memory [16] and the gated recurrent unit [17], in this work, we focus on a relatively new class of models that hybridize RNNs for numerical integration of ordinary differential equations [6--9]. In this approach, the building blocks of the governing equations are connected through directed acyclic graph [18, Ch. 2] to form the RNN repeating cell. For the reduced-order physics-based model describing battery discharge, the RNN representation is illustrated in Fig. 1.

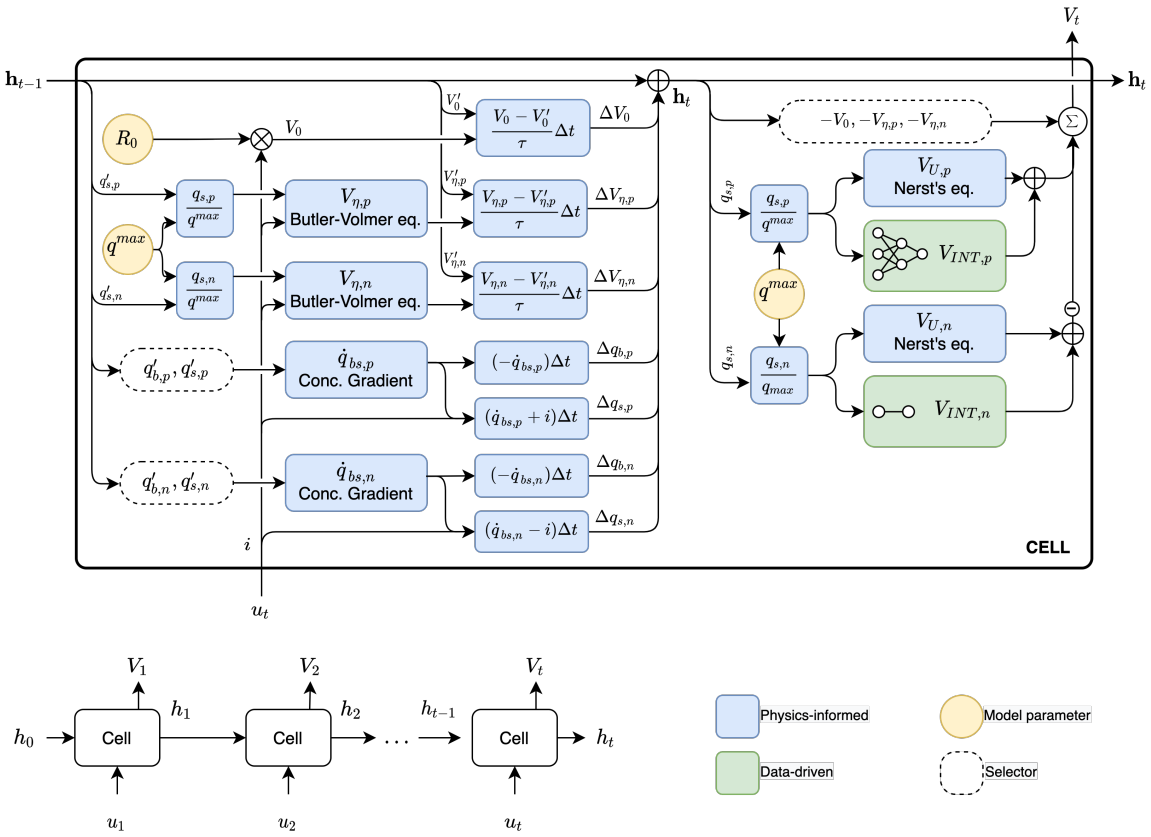

Fig. 1 Physics-informed RNN cell performing the state-space step-ahead prediction.

This RNN cell takes the state vector at the previous time step, $\boldsymbol{h}_{t-1}$ together with the input at the current time step, $\boldsymbol{u}_t$, and updates the state vector $\boldsymbol{h}_t$ and the output y_t. This RNN cell produces a one-step-ahead prediction of the entire state-space model such that

$$\boldsymbol{h} = [T, V_o, V_{\eta,n}, V_{\eta,p}, q_{b,n}, q_{s,n}, q_{b,p}, q_{s,p}]^\top, \qquad u = i, \qquad \text{and} \qquad y = V. \tag{10}$$

In the model previously discussed and illustrated in Fig. 1, the blue nodes are pure physics-blocks, which perform the same calculations of the physics-based model. The dashed-rounded white nodes show variable selectors. The green nodes are representative of the two data-driven models used to estimate the internal voltages, while the yellow circles represents the adjustable physical model parameters, q^{max} and R_0. The internal resistance R_0, the amount of available Li-ions q^{max}, and the internal voltages $V_{int,p}$ and $V_{int,n}$ need to be empirically adjusted based on observed data. With this mix of physics-based and data-driven nodes, the RNN model can capture the main trend of the battery discharge behavior through the physics, while the data-driven nodes reduce the discrepancies between predicted and observed outputs. Internal voltages $V_{int,p}$ and $V_{int,n}$ are modeled through multi-layer perceptrons (MLPs):

$$V_{int,n} = \text{MLP}_n(x_n;\, \mathbf{w}_n, \mathbf{b}_n) \qquad \text{and} \qquad V_{int,p} = \text{MLP}_p(x_p;\, \mathbf{w}_p, \mathbf{b}_p), \tag{11}$$

where $\mathbf{w}_n$, $\mathbf{b}_n$, $\mathbf{w}_p$, and $\mathbf{b}_p$, are MLP parameters.

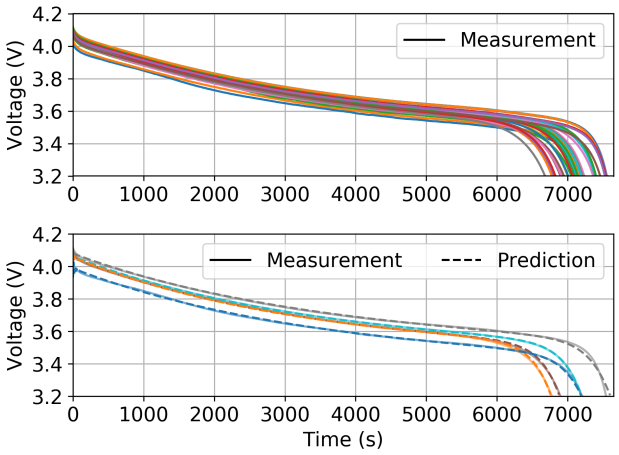

Fig. 2 Constant-loading discharge samples curves used for training (top panel) and examples of model predictions (bottom panel). The solid curves underneath the dashed curves are the ground truth curves used for model performance assessment.

IV. Results and Discussion

Our implementation is all done in TensorFlow* using the Python application programming interface (version 2.3). First, we trained our hybrid physics-informed neural network, which simultaneously optimizes the values of q^{max}, R_0, and the MLP parameters ($\mathbf{w}_n$, $\mathbf{b}_n$, $\mathbf{w}_p$, and $\mathbf{b}_p$). We chose to do so using the constant-loading data available in [10]. We extracted the first 3 constant-loading discharge curves from each of the 12 batteries in the data set. Each curve was generated with a current draw of 1 A from the fully charged condition of 4.2 V down to a value of 3.2 V, when the tests stopped. Then, we used the mean squared error as loss function Λ:

$$\Lambda = \frac{1}{N}\left(\mathbf{V} - \hat{\mathbf{V}}\right)^T \left(\mathbf{V} - \hat{\mathbf{V}}\right), \tag{12}$$

where N is the number of observations, vector $\mathbf{V}$ contains the observed battery voltages over time, and $\hat{\mathbf{V}}$ contains the predicted battery voltages by the physics-informed neural network. We trained our model with the Adam optimizer [19] set with a learning rate of 5×10^{-3} for 3000 epochs. All other Adam parameters were kept equal to their default values. Figure 2 summarizes the training results by contrasting the observed data and model predictions.

Once the hybrid physics-informed neural network model is trained with constant loading, we use it to make predictions at random loading conditions (also available in [10]). As opposed to reference constant loading, random loading better approximates the realistic battery usage. Figure 3 shows the prediction of the first random-loading discharge curves, after the batteries were tested in constant-loading conditions. For most batteries the predictions are very accurate, except for battery #1, that reportedly had problems in much of the recorded data.

From the engineering understanding of how these batteries operate, we know that over time, as the batteries accumulate cycles, the amount of available Li-ions q^{max} decreases while the internal resistance R_0 increases. The internal voltages $V_{int,p}$ and $V_{int,n}$ curves do not change with usage. Therefore, if we keep performing constant loading cycles regularly, we could use that information for tracking q^{max} and R_0.

As a matter of fact, Fig. 4a shows battery capacity and q^{max} as a function of the cumulative energy provided by the battery. We used the constant-loading cycles (which were performed regularly) to estimate the q^{max} values shown on top of battery capacity values. The clear correlation can, in principle, allow us to model aging by modeling the decay of its two proxies (q^{max} and R_0) as a function of the past energy drawn. We also observe that up to 1 kWh, all batteries show a very narrow dispersion of the capacity and q^{max} drop, manifesting low inter-specimen variability. The curves then start diverging. Nevertheless, battery capacity and q^{max} trends remain highly correlated. Once q^{max} and R_0 are tracked, predictions for random discharge cycles are expected to improve. Figure 4b illustrates the impact in one of the random-discharge cycle data. The bias in the model prediction due to the misestimation of q^{max} and R_0 is removed once these parameters are updated.

*www.tensorflow.org

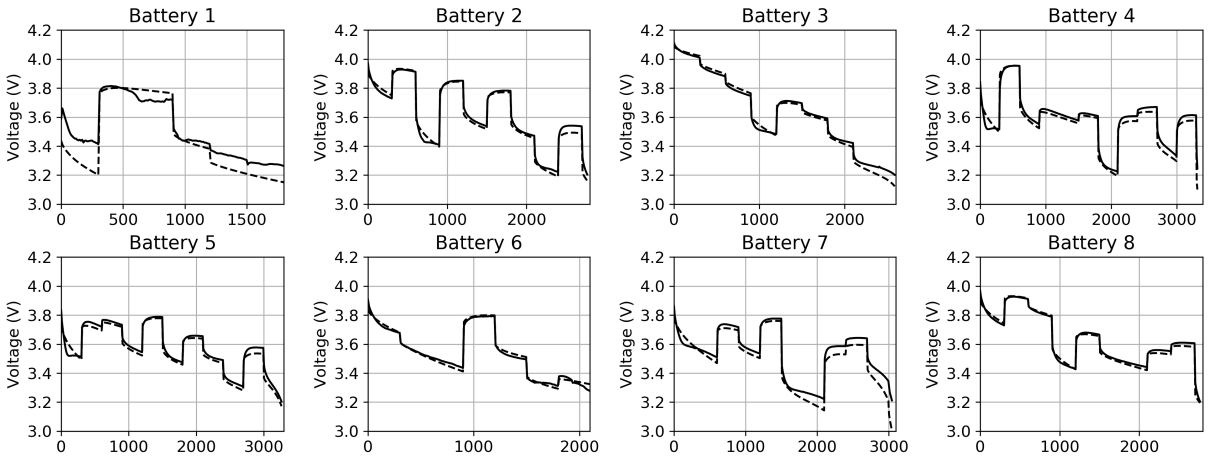

Fig. 3 Prediction of first random-loading discharge curves for batteries 1 to 8 from model trained only with reference discharge curves (constant load).

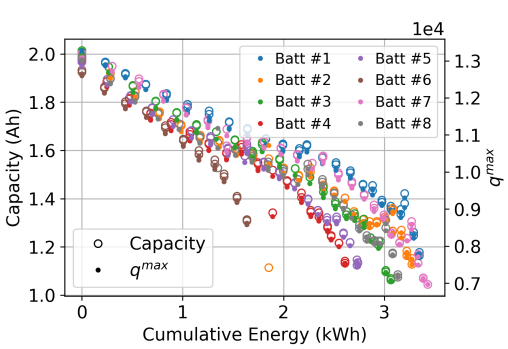

(a) Decrease in maximum capacity (left-vertical axis) and q^{max} (right-vertical axis) as a function of the cumulative energy.

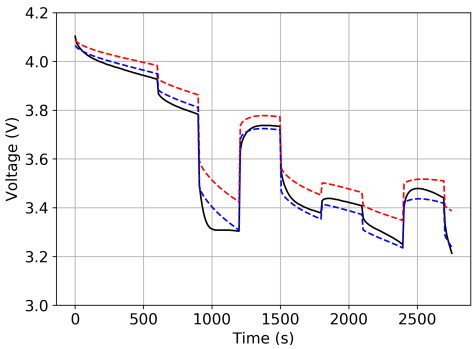

(b) Model voltage prediction under random input current loading before and after update the model parameters (q^{max}, R_0). The black curve is the observed data, the red curve is the prediction with outdated model parameters (RMSE 8.1e-02) and the blue curve is the prediction with updated model parameters (RMSE 3.1e-02)

Fig. 4 Variation of q^{max} as batteries accumulate loading cycles.

V. Summary and Future Work

We proposed a hybrid physics-informed neural network model for Li-ion battery discharge as well as aging prediction. The methodology blends physics-based models with the capability of machine learning algorithms to learn from data, thus providing a flexible model yet constrained by physics.

The results we showed here suggest that the hybrid model can successfully represent voltage discharge cycles under constant- and random-loading conditions after being trained with a few sample discharge curves. That same model can also track the aging of the battery over time by updating the estimates of the parameters q^{max} and R_0, which were used as proxies of the inner degradation phenomena of the batteries.

However, the ability to predict the remaining time to discharge of a single cycle, as well as the ability to track aging, depend upon several reference discharge cycles. That means several discharge curves obtained at different stages of the battery life using constant- and low-loading conditions. The need for such reference discharge cycles clearly has a negative impact on the application and deployment of the model in real-life operations; the parameter pair (q^{max}, R_0) should be re-calibrated by executing a reference discharge cycle on each battery at regular intervals. This means interrupt operations by taking the battery out of the fleet, perform the necessary reference-discharge test, and reintroduce the battery into the fleet.

As topic of future research, we suggest addressing the need for reference cycles and propose a methodology to update the aging parameter pair (q^{max}, R_0) using random-loading discharge curves. If such re-calibration stages during the aging stage are eliminated, the hybrid model could be applied to batteries operating in the field and learn the new values of q^{max} and R_0 as the battery is being used, without the need to disrupt operations. Another important research topic is how the hybrid model can account for uncertainty in the output voltage as well as future capacity drop. As a result, the parameters of the hybrid model would be defined by probability distributions instead of deterministic values, thus making the application of the approach look more attainable, as the aging predictions would be accompanied by confidence intervals.

Acknowledgments

This work was supported by the System-Wide Safety (SWS) project under the Airspace Operations and Safety Program within the NASA Aeronautics Research Mission Directorate (ARMD).

References

[1] Friedrich, C., and Robertson, P. A., ''Hybrid-electric propulsion for aircraft,'' *Journal of Aircraft*, Vol. 52, No. 1, 2015, pp. 176--189.

[2] Madavan, N., Heidmann, J., Bowman, C., Kascak, P., Jankovsky, A., and Jansen, R., ''A NASA perspective on electric propulsion technologies for commercial aviation,'' *Proceedings of the Workshop on Technology Roadmap for Large Electric Machines, Urbana-Champaign, IL, USA*, 2016, pp. 5--6.

[3] Russell, J., ''NASA, U.S. Industry Aim to Electrify Commercial Aviation,'' , October 2019. URL `https://www.nasa.gov/feature/glenn/2019/nasa-us-industry-aim-to-electrify-commercial-aviation`.

[4] Daigle, M. J., and Kulkarni, C. S., ''Electrochemistry-based battery modeling for prognostics,'' *Annual Conference of the Prognostics and Health Management Society*, PHM Society, New Orleans, USA, 2013, p. 13 pages.

[5] Karthikeyan, D. K., Sikha, G., and White, R. E., ''Thermodynamic model development for lithium intercalation electrodes,'' *Journal of Power Sources*, Vol. 185, No. 2, 2008, pp. 1398--1407.

[6] Nascimento, R. G., and Viana, F. A. C., ''Cumulative Damage Modeling with Recurrent Neural Networks,'' *AIAA Journal*, Online First, 2020. doi:10.2514/1.J059250, URL `https://arc.aiaa.org/doi/10.2514/1.J059250`.

[7] Dourado, A., and Viana, F. A. C., ''Physics-informed neural networks for missing physics estimation in cumulative damage models: a case study in corrosion fatigue,'' *ASME Journal of Computing and Information Science in Engineering*, Vol. 20, No. 6, 2020, p. 061007 (10 pages). doi:10.1115/1.4047173, URL `https://doi.org/10.1115/1.4047173`.

[8] Yucesan, Y. A., and Viana, F. A. C., ''A physics-informed neural network for wind turbine main bearing fatigue,'' *International Journal of Prognostics and Health Management*, Vol. 11, No. 1, 2020, pp. 27--44. URL `http://www.phmsociety.org/node/2736`.

[9] Nascimento, R. G., Fricke, K., and Viana, F. A. C., ''A tutorial on solving ordinary differential equations using Python and hybrid physics-informed neural networks,'' *Engineering Applications of Artificial Intelligence*, Vol. 96, 2020, p. 103996. doi:10.1016/j.engappai.2020.103996, URL https://www.sciencedirect.com/science/article/pii/S095219762030292X.

[10] Saha, B., and Goebel, K., ''Battery data set,'' NASA Ames Research Center, Retrieved 11 May 2020, 2007. URL http://ti.arc.nasa.gov/project/prognostic-data-repository.

[11] Bole, B., Kulkarni, C., and Daigle, M., ''Randomized battery usage data set,'' *NASA AMES prognostics data repository*, Vol. 70, 2014.

[12] Bole, B., Kulkarni, C. S., and Daigle, M., ''Adaptation of an electrochemistry-based Li-ion battery model to account for deterioration observed under randomized use,'' *Annual Conference of the Prognostics and Health Management Society*, PHM Society, 2014, p. 9 pages.

[13] Pearlmutter, B. A., ''Learning state space trajectories in recurrent neural networks,'' *Neural Computation*, Vol. 1, No. 2, 1989, pp. 263--269. doi:10.1162/neco.1989.1.2.263.

[14] Aussem, A., ''Dynamical recurrent neural networks towards prediction and modeling of dynamical systems,'' *Neurocomputing*, Vol. 28, No. 1-3, 1999, pp. 207--232. doi:10.1016/S0925-2312(98)00125-8.

[15] Goodfellow, I., Bengio, Y., and Courville, A., *Deep Learning*, MIT Press, 2016. URL http://www.deeplearningbook.org.

[16] Hochreiter, S., and Schmidhuber, J., ''Long short-term memory,'' *Neural Computation*, Vol. 9, No. 8, 1997, pp. 1735--1780. doi:10.1162/neco.1997.9.8.1735.

[17] Cho, K., Van Merriënboer, B., Gulcehre, C., Bahdanau, D., Bougares, F., Schwenk, H., and Bengio, Y., ''Learning phrase representations using RNN encoder-decoder for statistical machine translation,'' *arXiv preprint arXiv:1406.1078*, 2014.

[18] Barber, D., *Bayesian Reasoning and Machine Learning*, Cambridge University Press, 2012.

[19] Kingma, D. P., and Ba, J., ''Adam: A method for stochastic optimization,'' *arXiv preprint arXiv:1412.6980*, 2014.